Measurement of Partial-Wave Contributions in $pp \to pp\pi^0$

H. O. Meyer, J. T. Balewski, J. Doskow, R. E. Pollock, B. v. Przewoski, T. Rinckel, P. Thörngren-Engblom, and A. Wellinghausen
Department of Physics and Cyclotron Facility, Indiana University, Bloomington, Indiana 47405

W. Haeberli, B. Lorentz, F. Rathmann,* B. Schwartz, and T. Wise
University of Wisconsin-Madison, Madison, Wisconsin 53706

W. W. Daehnick and Swapan K. Saha†
Department of Physics and Astronomy, University of Pittsburgh, Pittsburgh, Pennsylvania 15260

P. V. Pancella
Western Michigan University, Kalamazoo, Michigan 49008
(Received 26 July 1999)

We report a measurement of the spin-dependent total cross section ratios $\Delta\sigma_{\mathrm{T}}/\sigma_{\mathrm{tot}}$ and $\Delta\sigma_{\mathrm{L}}/\sigma_{\mathrm{tot}}$ of the $pp \to pp\pi^0$ reaction between 325 and 400 MeV. The experiment was carried out with a polarized internal target in a storage ring. Nonvertical beam polarization was obtained by the use of solenoidal spin rotators. Near threshold, the knowledge of both spin-dependent total cross sections is sufficient to deduce the strength of certain participating partial waves, free of any model.

PACS numbers: 24.70.+s, 25.10.+s, 29.20.Dh, 29.25.Pj

We present a measurement of $\Delta\sigma_{\mathrm{T}}/\sigma_{\mathrm{tot}}$ and $\Delta\sigma_{\mathrm{L}}/\sigma_{\mathrm{tot}}$ for the $pp \to pp\pi^0$ reaction. The quantity $\Delta\sigma_{\mathrm{T}}$ (or $\Delta\sigma_{\mathrm{L}}$) equals the difference between the total cross sections measured with opposite and parallel, transverse (or longitudinal) beam and target polarizations, while σ_{tot} is the (unpolarized) total cross section. At threshold a single partial wave ($^3P_0 \to {}^1S_0$, $l = 0$) dominates. As the bombarding energy is increased other partial waves become significant. In the following, we will demonstrate how the results of the present experiment can be used to gain information on these higher partial waves, making it possible to test theoretical models selectively.

The reaction amplitude for pion production in the nucleon-nucleon (NN) system may be separated into contributions with definite angular momentum. These partial-wave amplitudes are labeled with the quantum numbers of the final state $(^{2S+1}L_J, l)_j$, where S, L, and J are the spin, angular momentum, and total angular momentum of the NN pair, l is the angular momentum of the pion, and j is the total angular momentum of the final state. The initial-state quantum numbers $\mathcal{S}$, $\mathcal{L}$, and $\mathcal{J}$ are related to those of the final state by angular momentum, parity, and isospin conservation.

It is useful to define cross sections $^{2S+1}\sigma_m$ which partition the total cross section σ_{tot} according to the initial NN spin, S, and its projection, m, onto the direction of the incident momentum. The three possible contributions $^1\sigma_0$, $^3\sigma_0$, and $^3\sigma_1$ are related to the observable quantities by [1]

$$\begin{aligned} {}^1\sigma_0 &= \sigma_{\mathrm{tot}} + \Delta\sigma_{\mathrm{T}} + \tfrac{1}{2}\Delta\sigma_{\mathrm{L}}\,, \\ {}^3\sigma_0 &= \sigma_{\mathrm{tot}} - \Delta\sigma_{\mathrm{T}} + \tfrac{1}{2}\Delta\sigma_{\mathrm{L}}\,, \\ {}^3\sigma_1 &= \sigma_{\mathrm{tot}} - \tfrac{1}{2}\Delta\sigma_{\mathrm{L}}\,. \end{aligned} \tag{1}$$

Because, near threshold, the relative kinetic energies between the particles in the final state are small, the angular momenta L and l are either 0 or 1, giving rise to the possible final states $Ll = Ss, Sp, Ps$, or Pp. A list of possible $pp \to pp\pi^0$ amplitudes can easily be constructed, taking into account the negative parity of the pion, as well as conservation of angular momentum and isospin. From this list, one sees that the Sp final state is not allowed, that only initial-state singlets ($^1\sigma_0$) contribute to Ps final states, that ($^3\sigma_1$) contributes only to Pp, and that ($^3\sigma_0$) may contribute to both Ss and Pp. Assuming that there are no final states other than Ss, Ps, and Pp, we require that $\sigma_{\mathrm{tot}} = \sigma_{Ss} + \sigma_{Ps} + \sigma_{Pp}$ where σ_{Ll} is the total cross section to a certain final state, Ll. We can then summarize the above in the following way:

$$\begin{aligned} {}^1\sigma_0 &= 4\sigma_{Ps}\,, \\ {}^3\sigma_0 &= 4(\sigma_{Ss} + \hat{\sigma}_{Pp})\,, \\ {}^3\sigma_1 &= 2(\sigma_{Pp} - \hat{\sigma}_{Pp})\,. \end{aligned} \tag{2}$$

Here, σ_{Pp} and $\hat{\sigma}_{Pp}$ represent two different combinations of Pp amplitudes. The term $\hat{\sigma}_{Pp}$ is needed in $^3\sigma_0$ because $S = 1$, $m = 0$ initial states can lead to Ss *and* Pp final states. Since the term $\hat{\sigma}_{Pp}$ does not contribute to the total cross section, it must also appear in $^3\sigma_1$. Combining Eqs. (1) and (2), we arrive at the useful relation

$$\frac{\sigma_{Ps}}{\sigma_{\mathrm{tot}}} = \frac{1}{4}\left(1 + \frac{\Delta\sigma_{\mathrm{T}}}{\sigma_{\mathrm{tot}}} + \frac{1}{2}\,\frac{\Delta\sigma_{\mathrm{L}}}{\sigma_{\mathrm{tot}}}\right), \tag{3}$$

which states that the probability to form a Ps final state can be deduced, free of any model, from the observables of

this experiment. A similar equation for $(\sigma_{Pp} - \hat{\sigma}_{Pp})/\sigma_{\rm tot}$ follows easily from Eqs. (1) and (2).

The experiment discussed here was carried out with the Indiana Cooler. Protons from the cyclotron were stack injected into the ring at 197 MeV, reaching an orbiting current of several 100 μA within a few minutes. The beam was then accelerated to the energies listed in Table I. After typically 10 min of data taking, the remaining beam was discarded, and the cycle was repeated.

The target and detector used for this experiment are the same as described in Ref. [2], and a detailed account of the apparatus can be found in Ref. [3]. The internal polarized target consisted of an open-ended 25 cm long storage cell of 12 mm diam and 25 μm wall thickness. The cell is coated with Teflon to avoid depolarization of atoms colliding with the wall. During data taking, the target polarization $\vec{Q}$ is changed every 2 s pointing in sequence, up, down ($\pm y$), left, right ($\pm x$), and along, opposite to the beam direction ($\pm z$). The magnitude of the polarization is the same within ± 0.005 for all orientations [4,5].

The detector arrangement consists of a stack of scintillators and wire chambers, covering a forward cone with a 30° opening angle. The scintillators are capable of stopping protons from $pp \to pp\pi^0$, thus measuring their energy. From the time of flight and the relative energy deposited in the layers of the detector, the outgoing charged particles are identified as protons. From the direction and energy of the two protons in the final state, the mass m_x of the undetected particle is calculated. For an event of interest, this mass has to equal the π^0 mass within the mass resolution of the experiment [2]. Background arises from reactions in the walls of the target cell [3] and, to a lesser degree, from a $\approx 1\%$ impurity in the target gas. Background is rejected by a condition on the relative angles of the detected protons and by a cut on the transverse distribution of the reaction vertices. A measurement with a nitrogen target matches the shape of the m_x distribution seen with the H target, except for the π^0 peak, and is used to subtract background which remains under the π^0 mass peak (between 5% and 10%). Within statistics, the background shows no spin dependence. The validity of the background subtraction was tested by varying the range of accepted masses m_x.

Nonvertical beam polarization is achieved by two spin-rotating solenoids located in nonadjacent sections of the six-sided Cooler. The vertical and longitudinal components of the beam polarization $\vec{P}$ at the target are about equal, with a small sideways component, while its magnitude was typically $|\vec{P}| \sim 0.6$. Since the solenoid fields are fixed in strength, the exact polarization direction depends on beam energy after acceleration. Only either the vertical or the longitudinal component contributes to the total cross section, depending on the orientation of the target polarization. In alternating measurement cycles, the sign of the beam polarization is reversed. More details on the preparation of nonvertical beam polarization in a storage ring can be found in Refs. [3,5].

Data are acquired for all twelve possible polarization combinations of beam $(+,-)$ and target $(\pm x, \pm y, \pm z)$. The known spin correlation coefficients of proton-proton elastic scattering [6] are used to monitor beam and target polarization, concurrently with the acquisition of $pp \to pp\pi^0$ events. To this end, coincidences between two protons exiting near $\Theta_{\rm lab} = 45°$ are detected by two pairs of scintillators placed behind the first wire chamber at azimuthal angles $\pm 45°$ and $\pm 135°$. From this measurement, the products $P_y Q_y$ and $P_z Q_z$ of beam and target polarization are deduced. Evaluating the cross ratio of the four $pp \to pp\pi^0$ yields with $\pm P$ and $\pm Q_y$, dividing by the measured $P_y Q_y$, results in $\Delta\sigma_{\rm T}/\sigma_{\rm tot}$. Analogously, $\Delta\sigma_{\rm L}/\sigma_{\rm tot}$ follows from the yields with $\pm P$ and $\pm Q_z$, using the measured $P_z Q_z$.

At 375 and 400 MeV, two data runs, separated by five months, were combined. The detector acceptance is less than 100% because of a hole in the center of the detector stack which accommodates the circulating beam, and excludes particles with $\Theta_{\rm lab} < 5°$. The resulting loss of events (about 30% at the lowest energy) is taken into account by applying a correction. This correction is small since it arises only from the difference in detector acceptance for the Ss, Ps, and Pp final states. It is straightforward to calculate the correction as a function of the size of the hole and to test this prediction against the data by artificially increasing the size of the hole in replay. The applied corrections were between 0.009 and 0.058 for $\Delta\sigma_{\rm T}/\sigma_{\rm tot}$, and between 0.007 and 0.030 for $\Delta\sigma_{\rm L}/\sigma_{\rm tot}$.

The final results are listed in Table I. The errors include counting statistics and an uncertainty for background subtraction and hole correction. The latter two were estimated

TABLE I. Bombarding energy T, maximum pion center-of-mass momentum η in units of the pion mass, integrated luminosity, the products $P_y Q_y$ and $P_z Q_z$ of beam and target polarization, and the measured $\Delta\sigma_{\rm T}/\sigma_{\rm tot}$ and $\Delta\sigma_{\rm L}/\sigma_{\rm tot}$ are listed. Column 7 lists the values for $\Delta\sigma_{\rm T}/\sigma_{\rm tot}$ from this experiment (column 6) combined with the results from an earlier measurement with purely vertical beam polarization [2].

T MeV	η	$\int L dt$ $(\text{nb})^{-1}$	$P_y Q_y$	$P_z Q_z$	$\Delta\sigma_T/\sigma_{\rm tot}$ This expt.	$\Delta\sigma_{\rm T}/\sigma_{\rm tot}$ Incl. [2]	$\Delta\sigma_L/\sigma_{\rm tot}$ This expt.
325.6	0.560	3.0	0.333(2)	0.296(3)	-1.155 ± 0.106	-1.078 ± 0.063	1.623 ± 0.116
350.5	0.707	1.4	0.316(3)	0.267(5)	-0.524 ± 0.099	-0.484 ± 0.067	1.277 ± 0.119
375.0	0.832	4.1	0.333(2)	0.266(4)	-0.239 ± 0.039	-0.274 ± 0.021	0.676 ± 0.049
400.0	0.948	1.1	0.289(4)	0.203(8)	-0.088 ± 0.065	-0.076 ± 0.038	0.590 ± 0.093

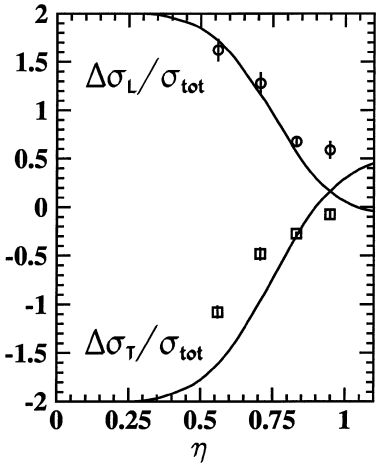

FIG. 1. The $pp \to pp\pi^0$ spin-dependent total cross sections $\Delta\sigma_T/\sigma_{tot}$ (column 7 in Table I) and $\Delta\sigma_L/\sigma_{tot}$ (column 8) as a function of η, the maximum pion center-of-mass momentum in units of the pion mass. The curves represent the predictions by the Jülich meson-exchange model [7].

by a reasonable variation ($\pm 25\%$) in the amount of background and in the size of the hole correction. The $\Delta\sigma_T/\sigma_{tot}$ results from this experiment were consistent with those obtained in an earlier experiment [2]. The weighted averages of the two data sets are shown in column 7 of Table I. The data in the last two columns of Table I represent all experimental information on $pp \to pp\pi^0$ spin-dependent total cross sections and are shown in Fig. 1.

Most of the recent theoretical work on $pp \to pp\pi^0$ so far deals with the lowest partial wave (Ss). An exception is the meson-exchange model of the Jülich group [7] which contains the higher partial waves needed to address polarization observables. This calculation includes off-shell pion rescattering and the exchange of heavy mesons, and provides a good fit to the Ss part of the total cross section close to threshold, or for $\eta < 0.5$, where η is the maximum center-of-mass pion momentum divided by the π^0 mass. The agreement is not as good for the polarization observables measured here (Fig. 1) which are sensitive to contributions from Ps and Pp partial waves.

As pointed out in the first part of this paper, the present measurement allows a model-free statement about the Ps and Pp contributions to $pp \to pp\pi^0$. Equation (3) directly yields the relative Ps strength, σ_{Ps}/σ_{tot}. The result is shown in Fig. 2. The Ps strength is larger than that proposed by Złomańczuk *et al.* [8] (see below).

Phase space arguments together with the properties of spherical Bessel functions for small arguments lead to the expectation that σ_{Ps} is proportional to η^6. In order to test this prediction, we have to multiply our experimental σ_{Ps}/σ_{tot} by the total cross section. At $T = 325$ MeV an accurate value for the total cross section exists ($\sigma_{tot} = 7.70 \pm 0.26$ μb [9]). However, at higher energies data are few and often of poor quality, so new, accurate measurements of σ_{tot} between 0.3 and 1 GeV are certainly a much-needed addition to the $pp \to pp\pi^0$ database. For the present purpose we use a smooth approximation to the world's data, obtaining $\sigma_{tot} = 17$, 40, and 86 μb, for $T = 350$, 375, and 400 MeV, respectively. The resulting values for σ_{Ps} are shown in Fig. 3. The dashed line in Fig. 3 represents the fit with $\sigma_{Ps} = \eta^6(33.8 \pm 1.3)$ μb. The error of the scaling factor takes into account the errors of the data, and the uncertainty of σ_{tot} at 325 MeV. One can also combine the expressions for ${}^3\sigma_1$ in Eqs. (1) and (2) to obtain an equation for $(\sigma_{Pp} - \hat{\sigma}_{Pp})/\sigma_{tot}$ in terms of $\Delta\sigma_L/\sigma_{tot}$. Multiplying the result by σ_{tot} yields the Pp partial cross section, $\sigma_{Pp} - \hat{\sigma}_{Pp}$, shown in Fig. 4. The dashed line in Fig. 4 represents a fit with the expected energy dependence for Pp waves, $(\sigma_{Pp} - \hat{\sigma}_{Pp}) = \eta^8(53.9 \pm 3.4)$ μb. The solid lines in Figs. 3 and 4 are obtained with the Jülich meson-exchange model [7]. One sees that the Ps strength which, in this model, is dominated by the role of the Δ (a nucleon excited state) is underestimated by about a factor of 3 (Fig. 3), while for $(\sigma_{Pp} - \hat{\sigma}_{Pp})$ the discrepancy is less but the energy dependence is not correctly reproduced by the model (Fig. 4).

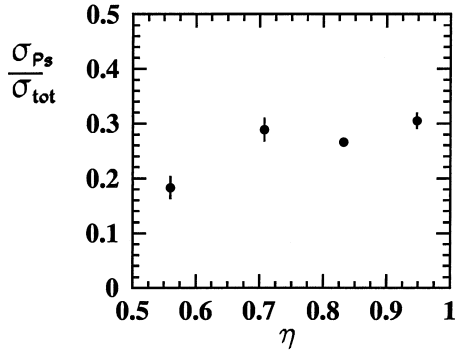

FIG. 2. Measured, relative Ps strength, σ_{Ps}/σ_{tot}, of the reaction $pp \to pp\pi^0$ as a function of η.

In the absence of polarization observables, some information on individual partial-wave contributions can be

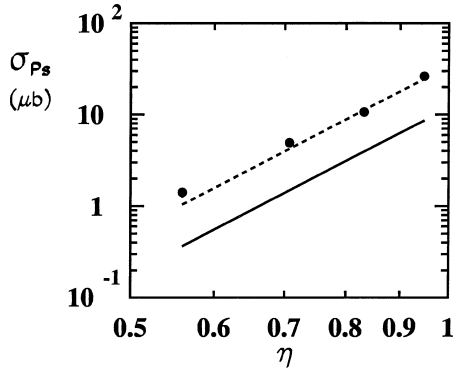

FIG. 3. The total cross section σ_{Ps} for $pp \to pp\pi^0$ as a function of η. The dashed line represents the best fit with σ_{Ps} proportional to η^6. The solid line is the Ps total cross section calculated from the Jülich meson-exchange model [7].

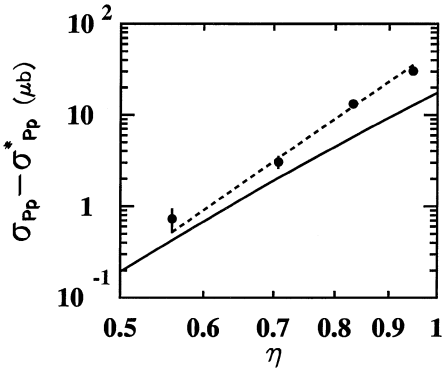

FIG. 4. The total cross section $\sigma_{Ps} - \hat{\sigma}_{Pp}$ for $pp \to pp\pi^0$ as a function of η. The dashed line represents the best fit with $\sigma_{Ps} - \hat{\sigma}_{Pp}$ proportional to η^8. The solid line is the prediction of the Jülich meson-exchange model [7].

extracted from a measurement of the (unpolarized) cross section as a function of the relative energy of the two nucleons in the final state, assuming that the corresponding energy distributions of single partial waves are known. As our data indicate, the Ps and Pp partial waves, up to 400 MeV, vary with energy like η^6 and η^8, respectively, but the energy dependence of the Ss partial wave is dominated by the final-state interaction, and thus requires model-dependent input. Such an analysis has been carried out for $pp \to pp\pi^0$ at 310 MeV ($\eta = 0.451$) [8]. In that work a significant contribution was found from an Sd-Ss interference term. This conclusion was reached, however, setting $\sigma_{Ps} = 0$, while from the present data, using an η^6 energy dependence, we estimate that, at 310 MeV, σ_{Ps} contributes about 6% to σ_{tot}.

In summary, we have measured both spin-dependent total cross sections in $pp \to pp\pi^0$. These polarization observables allow a model-free determination of individual partial-wave contributions. The only assumption is that higher partial waves (Ds, Dp, etc.) are negligible (calculations [10] indicate that these contributions are below the level of 1% of σ_{tot}, up to $\eta = 1.5$). We show in an example that this can provide a test of individual components of a model (Figs. 3 and 4). The availability of polarization observables is crucial when carrying out a partial-wave study, since an analysis based only on the unpolarized differential cross section is subject to model dependence.

We thank Dr. Ch. Hanhart for supplying us with the numerical values for the calculation shown in Figs. 1, 3, and 4. This work has been supported by the U.S. National Science Foundation under Grants No. PHY96-02872, No. PHY95-14566, No. PHY97-22556, and by the U.S. Department of Energy under Grant No. DOE-FG02-88ER40438.

*Present address: Forschungs Zentrum Jülich GmbH, 52425 Jülich, Germany.
†Permanent address: Bose Institute, Calcutta, 700009 India.

[1] S. M. Bilenky and R. M. Ryndin, Phys. Lett. **6**, 217 (1963).
[2] H. O. Meyer *et al.,* Phys. Rev. Lett. **81**, 3096 (1998).
[3] T. Rinckel *et al.,* Nucl. Instrum. Methods Phys. Res. (to be published).
[4] F. Rathmann *et al.,* Phys. Rev. C **58**, 658 (1998).
[5] B. Lorentz *et al. (*to be published).
[6] B. v. Przewoski *et al.,* Phys. Rev. C **58**, 1897 (1998).
[7] C. Hanhart, J. Haidenbauer, O. Krehl, and J. Speth, Phys. Lett. B **444**, 25 (1998).
[8] J. Złomańczuk *et al.,* Phys. Lett. B **436**, 251 (1998).
[9] H. O. Meyer *et al.,* Nucl. Phys. **A539**, 633 (1992).
[10] C. Hanhart, Ph.D. thesis, Bonn University, 1997.